# Grain-Boundary Structure Influenced by Li-addition in Gd-Doped Ceria

Kiminori Sato

**Abstract**— High resistive ionic transport at the grain boundary is one of the most decisive factors for designing sophisticated nanostructured electrolytes as oxide ceramics. Here, the grain boundary structures are specifically investigated for nanostructured electrolytes: ceria ($CeO_2$), Gd-doped ceria (GDC), and GDC with 3 mol % and 9 mol % Li doping (Li-GDC), by means of positron lifetime spectroscopy. The influence of Li addition on the grain boundary structures is discussed on the basis of our recent model with the space charge layer.

**Index Terms**— GDC, $CeO_2$, $Gd_2O_3$, Li-GDC, grain boundary, positron, space charge layer.

## 1 Introduction

Nanostructured electrolytes have gained an interest for potential application as environmentally-friendly solid state fuel cells owing to high performance at intermediate temperatures (773 K – 973 K) [1]. In rare-earth-doped ceria, as e.g., Gd-doped ceria (GDC) [2], an ionic conductivity occurs by migration of oxygen ions through oxygen vacancies produced by the substitution of $Ce^{4+}$ with $Gd^{3+}$. An availability of oxygen vacancies inside electrolytes is thus of significance for achieving the higher conductivity for oxygen ions [3]. It has been reported that the grain-boundary conductivity for rare-earth-doped ceria is lower than that of the bulk by several orders of magnitude [4]. The high resistive grain boundary for rare-earth doped ceria has been identified based on the results of impedance spectroscopy [4-5]. The impedance data are well explained by the space charge model, in which the grain boundary consists of a grain-boundary core and two adjacent space charge layers [4, 6-11]. In addition to that, cation phases have been often observed at the grain boundary due to dopant segregation by high-resolution transmission electron microscopy (TEM) [7, 12]. It has been thus believed that the high resistive grain boundary arises from the depletion of positively charged oxygen vacancies in the negative space charge layers [7].

A positron, anti-particle of electron, is a positively charged particle that can sensitively localize at the negatively charged spaces on an angstrom scale in materials. In metals, intermetallic compounds [13] and quasicrystals [14], satisfactory results have been given for the studies on lattice vacancies that are negatively charged relevant to the matrix due to missing of positive ion core. It has been demonstrated that the negatively charged part localized on polar elements in polymers is probed by positrons [15-16]. The size of open space can be investigated through the measurements of positron lifetimes by positron lifetime spectroscopy [13-16]. In the present study, the grain-boundary structures were studied for $CeO_2$ and GDC on an atomic scale by positron lifetime spectroscopy. GDC doped with different amount of Li (Li-GDC) was examined as well since Li is one of the effective sintering aids due to the capillary effect of liquid phase into the grain boundaries [18-19]. An influence of Li addition on the grain boundary structures is discussed on the basis of our recent model with the space charge layer [20].

• *Department of Environmental Sciences, Tokyo Gakugei University, Koganei, Tokyo 184-8501, Japan. E-mail: sato-k@u-gakugei.ac.jp*

## 2 Experiments

GDC was prepared using oxalate coprecipitation method [21-22]. The Ce-Gd nitrate solution mixed at a Gd molar ratio of ~ 0.2 was dropped into stirred oxalate acid solution to produce oxalate precipitates. The precipitates were calcined at 873 K for 1 h under the atmospheric condition to form oxides. Li-GDC was prepared by adding $LiNO_3$ into GDC with ethanol as dispersant so that 3 mol % and 9 mol % Li can be obtained, which are referred as Li-GDC1 and Li-GDC2, respectively, thereafter. The powder samples were compacted into pellets by uniaxial pressing with a pressure of 20 MPa and sintered at 873 K for 1 h in the air. The pellets of $CeO_2$ and $Gd_2O_3$ were prepared with the same procedure as that of GDC and sintered at 1073 K for 2 h in the air.

Positron lifetime spectroscopy was performed at room temperature. The positron source ($^{22}Na$), sealed in a thin foil of Kapton, was mounted in a sample-source-sample sandwich for the measurements. Positron lifetime spectra (~ $1 \times 10^6$ coincidence counts) were recorded with digital oscilloscope-based system, in which the time resolution of 190 ps full-width at half-maximum (FWHM) was achieved. The lifetime spectra were numerically analyzed using the POSITRONFIT code [23].

## 3 Results and Discussion

Table 1 lists the results of positron lifetime spectroscopy for $CeO_2$, GDC, Li-GDC1, and Li-GDC2 together with those of $Gd_2O_3$ and yttria-stabilized zirconia (s-YSZ) single crystal, which are similar materials of oxide family. In contrast with YSZ single crystal where a single component of positron lifetime corresponding to annihilation in the matrix is observed, two components of positron lifetime are obtained for $CeO_2$, GDC, Li-GDC1, Li-GDC2, and $Gd_2O_3$. The average positron

diffusion length in the YSZ single crystal without any trapping center is reported as $L_+$ = ~ 60 nm [24]. On the other hand, the present samples of $CeO_2$, GDC, and Li-GDC are polycrystalline materials that consist of the particle and the crystallite of minimum structural unit with structural perfection, as discussed in detail in our earlier paper [22]. As revealed by XRD experiments, the crystallite sizes of $CeO_2$, GDC, and Li-GDC are 18 nm, 14 nm, and 27 nm [20], which are by far smaller than the positron diffusion length in YSZ single crystal. Positrons implanted in the crystallites of $CeO_2$, GDC, Li-GDC, and $Gd_2O_3$ are thus expected to diffuse sufficiently to reach the grain boundaries, indicating that the positron annihilation sites are exclusively located at the grain boundaries. Besides the present GDC and Li-GDC, positron annihilation at the grain boundaries have been often reported for nanocrystal-embedded amorphous [14] and nanometer-sized polycrystal [26] so far.

TABLE 1
POSITRON LIFETIMES WITH THEIR RELATIVE INTENSITIES OBTAINED FOR $CeO_2$, GDC, AND TWO KINDS OF LI-GDC. THE DATA FOR $Gd_2O_3$ AND YSZ SINGLE CRYSTAL ARE PRESENTED FOR COMPARISON.

| Sample | $\tau_1$ [ps] | $I_1$ [%] | $\tau_2$ [ps] | $I_2$ [%] | $\tau_3$ [ps] | $I_3$[%] |
|---|---|---|---|---|---|---|
| $CeO_2$ | 183±2 | 90±2 | | | 441±6 | 10±2 |
| $Gd_2O_3$ | 193±3 | 72±2 | | | 551±6 | 28±2 |
| s-YSZ | 180±2 | 100 | | | | |
| GDC | | | 253±4 | 77±2 | 501±6 | 23±2 |
| Li-GDC | | | 225±3 | 87±2 | 332±5 | 13±2 |
| Li-GDC2 | | | 214±4 | 92±2 | 323±5 | 7±2 |

The shorter lifetimes $\tau_1$ of dominant components obtained for $CeO_2$ and $Gd_2O_3$ are close to that of YSZ single crystal, signifying the presence of tightly packed region as the grain-to-grain contact essentially identical to bulk. On the other hand, significantly longer lifetimes $\tau_2$ are obtained as dominant components for GDC, Li-GDC1, and Li-GDC2, which are attributable to positron annihilation in the space with the size of a few atoms. Further longer positron lifetimes $\tau_3$ for $CeO_2$, GDC, Li-GDC1, Li-GDC2 and $Gd_2O_3$ can be ascribed to the void-like open spaces created by lattice mismatching at the grain boundaries. The positron lifetime of 441 ps for $CeO_2$ increases up to 501 ps for GDC, indicating that the void-like open spaces at the grain boundaries are enlarged upon $Gd^{3+}$ doping into $CeO_2$. The positron lifetime of 501 ps for GDC decreases down to 332 ps for Li-GDC1, indicating the shrinkage of void-like open spaces upon $Li^+$ doping into GDC. This shrinkage effect is further enhanced with increasing Li addition up to 9 mol %. In the light of the fact that both the values of positron lifetime $\tau_3$ and its relative intensity $I_3$ for Li-GDC are smaller than those of GDC, an addition of Li significantly densifies the grain boundaries shrinking the void-like open spaces.

Positron is known to act as a highly sensitive probe of the angstrom-scale local spaces with negative charges. The observed annihilation spaces with the size of a few atoms located at the grain boundaries of GDC and Li-GDC are negatively charged. As clarified by our previous coincident Doppler broadening spectroscopy, the negatively charged spaces of GDC and Li-GDC are associated with Gd and Li at the grain boundaries, respectively. Our former study has further indicated that a small amount of lattice cation $Gd^{3+}$ with below the detection limit of XRD is heterogeneously distributed at the grain boundaries even after calcination [22]. The segregation of $Gd^{3+}$ to the grain boundaries creates positively charged local spaces, by which negatively charged spaces adjacent to them are formed. The cation of $Li^+$ added as sintering aid segregates to the grain boundaries being positively charged local spaces as observed by TEM earlier [19], which forms the negatively charged spaces adjacently. The higher relative intensity $I_2$ for Li-GDC1 and Li-GDC2 than that of GDC indicates that the negative charge for Li-GDC is more densely distributed than that of GDC.

The grain-boundary structures of CeO2, GDC, and Li-GDC have been modeled based on the results of positron lifetime and coincident Doppler broadening spectroscopy [20], as schematically shown in Fig. 1. The grain boundary of $CeO_2$ is composed of grain-to-grain contact and void-like open space, which are denoted as local atomic sites a and c, respectively. Upon Gd doping into $CeO_2$, the grain-boundary width expands owing to segregation of $Gd^{3+}$, disappearing the grain-to-grain contact and thus enlarging void-like open space. An addition of 3 mol % Li into GDC as sintering aid causes segregation of $Li^+$ into the grain boundary and narrows the width of grain boundary, shrinking the void-like open spaces. This effect could be enhanced by increasing Li addition up to 9 mol %. Segregation of $Gd^{3+}$ and $Li^+$ creates negatively charged spaces with the size of few atoms adjacently to the segregated cations, denoted as local atomic site b. These negatively charged spaces identified here are the origin of space charge layer, which has been discussed in the context of space charge theory for the grain-boundary conductivity.

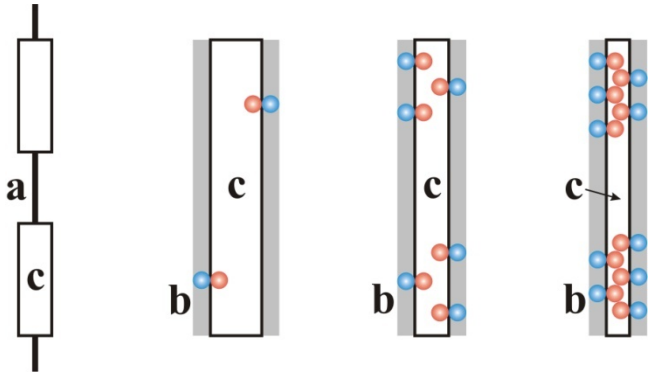


Fig. 1. Schematic illustrations of grain-boundary structures for $CeO_2$, GDC, and Li-GDC. The local atomic sites a, b, and c are identified by the present positron annihilation spectroscopy. The local atomic sites a and c correspond to grain-to-grain contact and void-like open space created by lattice mismatching, respectively. Red circles are positively charged local spaces caused by $Gd^{3+}$ and $Li^+$ segregates. Blue circles denoted as b are negatively charged spaces adjacent to the positive charges. Gray shadows are negative-space charge layers originated from the negatively charged spaces b.

## 4 Conclusion

The grain-boundary structures were studied for $CeO_2$, GDC, and Li-GDC by means of positron lifetime spectroscopy. The void-like open spaces created by lattice mismatching in addition to the grain-to-grain contacts essentially identical to the bulk were found at the grain boundaries for $CeO_2$. An addition of $Li^+$ as sintering aid significantly densifies the grain boundaries. This effect is further enhanced by an increase of Li addition. Both the cations of $Gd^{3+}$ and $Li^+$ segregate to the grain boundaries decreasing the grain-to-grain contacts and forming positively charged local spaces for GDC and Li-GDC, by which the negatively charged spaces adjacent to them are created. The angstrom-scale spaces with negative charge identified in the present study are the origin of space charge layer, which has been discussed in the context of space charge theory for the grain-boundary conductivity.

## Acknowledgment

The author is indebted to T. Kosaka (Tokyo Gakugei University) for supplying GDC samples. This work was partially supported by a Grant-in-Aid of the Japanese Ministry of Education, Science, Sports and Culture (Grant Nos. 25400318 and 25400319).

## References

[1] J. A. Kilner and C. D. Waters, "The effects of dopant cation-oxygen vacancy complexes on the anion transport properties of non-stoichiometric fluorite oxides.," Solid State Ionics, vol. 6, pp. 253-259, 1982.

[2] S. A. Acharya, V. M. Gaikwad, V. Sathe, and S. K. Kulkarni, "Influence of gadolinium doping on the structure and defects of ceria under fuel cell operating temperature," Appl. Phys. Lett. vol. 104, pp. 1135081-1135085, 2014.

[3] Ding Rong Ou, Toshiyuki Mori, Fei Ye, Tomoaki Kobayashi, Jin Zou, Graeme Auchterlonie, and John Drennan, "Oxygen vacancy ordering in heavily rare-earth-doped ceria," Appl. Phys. Lett., vol. 89, pp. 1719111-1719113, 2006.

[4] Hugo J. Avila-Paredes, Kwanghoon Choi, Chien-Ting Chen, and Sangtae Kim, "Dopant-concentration dependence of grain-boundary conductivity in ceria: A space-charge analysis," J. Mater. Chem., pp. 19, pp. 4837-4842, 2009.

[5] Taro Shimonosono, Yoshio Sakka, and Yoshihiro Hirata, "Electrical conductivity of Gd-doped ceria with nano-sized grain," Trans. Mater. Res. Soc. Jpn., vol. 34, pp. 555-559, 2009.

[6] Joachim Maier, "Space charge regions in solid two-phase systems and their conduction contribution—I. Conductance enhancement in the system ionic conductor-'inert' phase and application on AgC1: $Al_2O_3$ and AgC1: $SiO_2$," J. Phys. Chem. Solids, vol. 46, pp. 309-320, 1985.

[7] Xin Guo, Wilfried Sigle, Jürgen Fleig, Joachim Maier, "Role of space charge in the grain boundary blocking effect in doped zirconia," Solid State Ionics, vol. 154-155, pp. 555-561, 2002.

[8] Xin Guo and Rainer Waser, "Space charge concept for acceptor-doped zirconia and ceria and experimental evidences," Solid State Ionics, vol. 173, pp. 63-67, 2004.

[9] Xin Guo and Zaoli Zhang, "Grain Size Dependent Grain Boundary Defect Structure: Case of Doped Zirconia," Acta Mater., vol. 51, pp. 2539-2547, 2003.

[10] S. Azad, O. A. Marina, C. M. Wang, L. Saraf, V. Shutthanandan, D. E. McCready, A. El-Azab, J. E. Jaffe, M. H. Engelhard, C. H. F. Peden, and S. Thevuthasan, "Nanoscale effects on ion conductance of layer-by-layer structures of gadolinia-doped ceria and zirconia," Appl. Phys. Lett., vol. 86, pp. 1319061-1319063, 2005.

[11] Christian Kjølsetha, Harald Fjelda, Øystein Prytzb, Paul Inge Dahlc, 1, Claude Estournèsd, Reidar Haugsruda, Truls Norbya, "Space-charge theory applied to the grain boundary impedance of proton conducting $BaZr_{0.9}Y_{0.1}O_{3-\delta}$," Solid State Ionics, vol. 181, pp. 268-275, 2010.

[12] Zhi-Peng Li, Toshiyuki Mori, Graeme John Auchterlonie, Jin Zou, and John Drennan, "Direct evidence of dopant segregation in Gd-doped ceria," Appl. Phys. Lett., vol. 98, pp. 093104-0931043, 2011.

[13] K. Sato, H. Murakami, W. Sprengel, H.-E. Schaefer, Y. Kobayashi, "Nanocrystallization Mechanism of Amorphous $Fe_{78}B_{13}Si_9$," Appl. Phys. Lett., vol. 94, pp. 1719041-1719043, 2009.

[14] K. Sato, F. Baier, W. Sprengel, R. Würschum, and H.-E. Schaefer, "Study of an Order-Disorder Phase Transition on an Atomic Scale: The Example of Decagonal Al-Ni-Co Quasicrystals," Phys. Rev. Lett., vol. 92, pp. 1274031-12747034, 2004.

[15] K. Sato, K. Ito, K. Hirata, R.S. Yu, and Y. Kobayashi, "Intrinsic momentum distributions of positron and positronium annihilation in polymers," Phys. Rev. B, vol. 71, pp. 0122011-0122014, 2005.

[16] K. Sato, D. Shanai, Y. Hotani, T. Ougizawa, K. Ito, K. Hirata, and Y. Kobayashi, "Positronium formed by Recombination of Positron-Electron Pairs in Polymers," Phys. Rev. Lett., vol. 96, pp. 2283021-2283024, 2006.

[17] K. Sato, H. Murakami, K. Ito, K. Hirata, and Y. Kobayashi, "Probing the Elemental Environment around the Free Volume in Polymers with Positron Annihilation Age-Momentum Correlation Spectroscopy," Macromolecules, vol. 42, pp. 4853-4857, 2009.

[18] Jason D. Nicholas and Lutgard C. De Jonghe, "Prediction and evaluation of sintering aids for Cerium Gadolinium Oxide," Solid State Ionics, vol. 178, pp. 1187-1194, 2007.

[19] Tenglong Zhu, Ye Lin, Zhibin Yang, Dong Su, Shuguo Ma, Minfang Han, and Fanglin Chen, "Evaluation of $Li_2O$ as an efficient sintering aid for gadolinia-doped ceria electrolyte for solid oxide fuel cells," J. Powder Sources, vol. 261, pp. 255-263, 2014.

[20] Kiminori Sato, "Grain-boundary structures associated with ionic transport in Gd-doped Ceria nanostructured electrolyte," J. Phys. Chem. C, vol. 119, pp. 5734-5738, 2015.

[21] K. Higashi, K. Sonoda, H. Ono, S. Sameshima, and Y. Hirata, "Synthesis and sintering of rare-earth-doped ceria powder by the oxalate coprecipitation method," J. Mater. Res., vol. 14, pp. 957-967, 1999.

[22] Kiminori Sato, "Densification dynamics of Gadolinium-doped Ceria upon sintering," Jpn. J. Appl. Phys., vol. 51, pp. 0773011-0773014, 2012.

[23] P. Kirkegaard, and M. Eldrup, "Positronfit extended: A new version of a program for analysing position lifetime spectra," Computer Phys. Commun., vol. 7, pp. 401-409, 1974.

[24] R. I. Grynszpan, S. Saudé, L. Mazerolles, G. Brauer, and W. Anwand, "Positron depth profiling in ion-implanted zirconia stabilized with trivalent cations," Radiat. Phys. Chem., vol. 76, pp. 333-336, 2007.

[25] H. -E. Schaefer, R. Würschum, R. Birringer, H. Gleiter, "Structure of nanometer-sized polycrystalline iron investigated by positron lifetime spectroscopy," Phys. Rev. B, vo. 38, 9545-9554, 1988.